

# Dexhand : a Space qualified multi-fingered robotic hand

Maxime Chalon\*, Armin Wedler, Andreas Baumann, Wieland Bertleff, Alexander Beyer, Joerg Butterfaß, Markus Grebenstein, Robin Gruber, Franz Hacker, Erich Kraemer, Klaus Landzettel, Maximilian Maier, Hans-Juergen Sedlmayr, Nikolaus Seitz, Fabian Wappler, Bertram Willberg, Thomas Wimboeck, Gerd Hirzinger<sup>1</sup>, and Frederic Didot<sup>2</sup>

<sup>1</sup>*Institute of Robotics and Mechatronics, German Aerospace Center (DLR), Wessling, Germany*

<sup>2</sup>*Frederic Didot, European Space Agency (ESA)*

\**E-mail:Maxime.Chalon@dlr.de*

**Abstract**—Despite the progress since the first attempts of mankind to explore space, it appears that sending man in space remains challenging. While robotic systems are not yet ready to replace human presence, they provide an excellent support for astronauts during maintenance and hazardous tasks. This paper presents the development of a space qualified multi-fingered robotic hand and highlights the most interesting challenges. The design concept, the mechanical structure, the electronics architecture and the control system are presented throughout this overview paper.

## INTRODUCTION

Sending humans into space remains challenging and requires large efforts. The human intelligence is necessary to provide reactivity and adaptation that computer systems, especially the ones for space applications, are lacking. However, the risks and associated costs of sending human beings to outer space are a strong limiting factor. While robotic systems are not yet ready to replace humans, they provide an excellent support for astronauts during repetitive or hazardous tasks. Under control of a tele-manipulation system the robotic systems could replace many of the Extra Vehicular Activities (EVAs). Semi-autonomous control could also be used for simple routine tasks.

The European Space Agency (ESA) is currently investigating solutions in order to bring teleoperated systems to the International Space Station (ISS).

The equipment and the tools on board of the ISS are designed for humans. Hence, they are meant to be used with hand and arm. Moreover, if used in a tele-manipulation scenario, the mapping from the operator to the robotic system must be as intuitive as possible. It minimizes the learning time, the user fatigue and improves execution speed. Upon those arguments, ESA decided to develop an EVA capable hand/arm system.

Similar projects are led by JPL, with the hand of Robonaut [1], or at the University of Laval, with the under-actuated SARAH hand [2].

This paper presents the development of an EVA qualified dexterous robotic hand by the German Aerospace Agency (DLR) at the Institute of Robotics and Mechatronics (Fig.1). The project will be presented based on the Critical Design

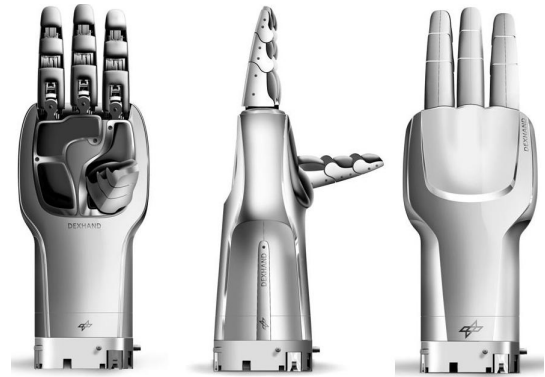


Fig. 1. CAD model of the hand

Review stage. It is an overview of the technical decisions in the mechatronic design including the holistic view of the mechanics, electronics and software systems, subject to the constraints of outer space operation.

The first part presents the main requirements for the systems and explains how the general concepts have been selected. The second part "reveals" the mechanical structure, the tendon actuation system and the torque sensor implementation. The third part concentrates on the space-related electronic design features and on the critical issue of heat dissipation. The fourth part gives an overview of the control system, controller architecture and software architecture.

## I. SYSTEM OVERVIEW

The development of a torque controlled multi-fingered hand is a domain in which the DLR has a long standing history [3]–[6]. However, providing a space compliant product is a complex multi-domain problem. The Dexhand is designed to be able to perform a set of generic tasks that are space oriented. For example, the removal of a multi layered insulation (MLI) cover or the manipulation of an automatic screw driver. This section presents how the design concept and the architecture of the hand are selected based on the hand capability requirements.

Requirement:	OPS-1
<p>The DEXHAND shall be able to grasp the following EVA tools:</p> <ul style="list-style-type: none"> <li>• Pliers, and support their operations</li> <li>• Scissors, and support their operations</li> <li>• Small cutter and support ist operations</li> <li>• Brush, and support ist operations</li> <li>• Hammer, and support ist operations</li> <li>• Scoop, and support ist operations</li> <li>• Cutter, and support ist operations</li> <li>• Tether(s), and support its operations</li> <li>• Allen wrench, and support ist operations</li> <li>• Pistol grip tool (automatic screw driver) and support its trigger switch actuation</li> </ul> <p>Comment: Successful operation of the tools implies force closure of the grasp. Note that preferably form closure should be achieved.</p>	

Fig. 2. Requirements for the Dexhand (subset)

### A. Requirements

The design constraints of the Dexhand are driven by its requirements. Some constraints are purely technical: operating temperature, maximum fingertip forces, joint velocity, but others are functional, such as grasping and operating a pistol grip tool (a space version of an electric driller). The desired capabilities must be translated into technical requirements that result in a trade-off between system complexity, capabilities, reliability, volume, weight and cost. Figure 2 reports an example of a top level functional requirement.

### B. Concepts

In the robotic community, hands are ranging from the simplest grippers to the most advanced biomimetic devices. The design space (ie. the possible design solutions) of hands is extremely large, therefore, the first part of the project was to select a concept that would fit to the initial requirements. Examples of the most important parameters that must be selected are:

- Number of fingers
- Number of degrees of freedom (DoF) per finger
- Number of actuated DoFs
- Placement of the fingers within the hand
- Shape of the fingertips
- Size of the fingers

Certainly, each finger DoF brings more capabilities but increases the number of parts. The use of multiple small actuators, instead of a single large actuator, increases the capabilities to distribute power losses, might provide redundancy, and usually provides a better form factor. However, the raw power density is reduced. The control complexity and the number of sensors must also be increased in order to take advantage of the available degrees of freedom.

The principle parameters are selected based on the manipulation experience gathered with the DLR Hand II and DLR/HIT hand. A parameter refinement is done by simulating grasps with each object of the EVA tool list.

For example, in order to perform trigger actuation of the pistol grip tool, while maintaining tool stability, it appears that at least three fingers are required.

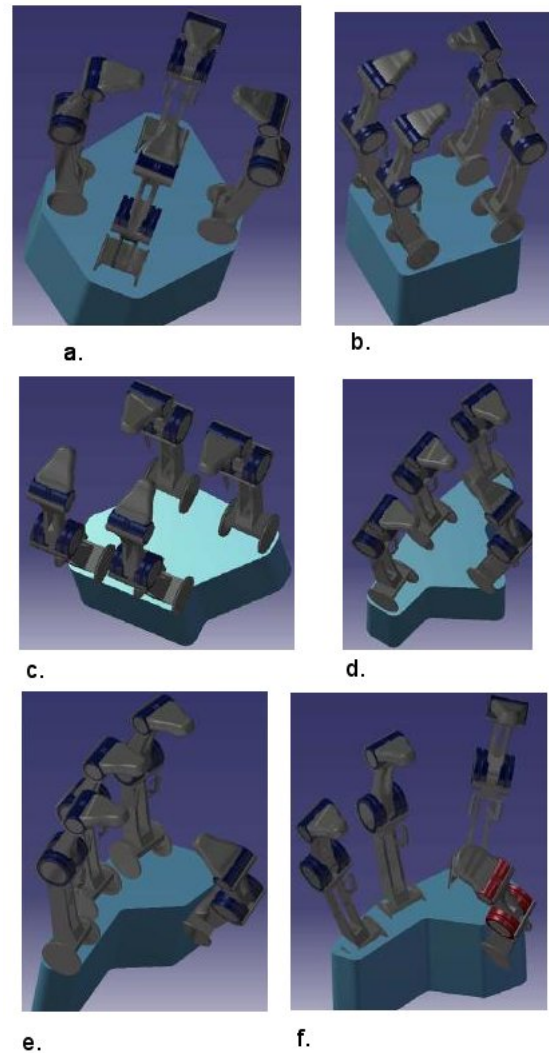


Fig. 3. Examples of four finger configurations. Some general remarks about the configurations are: a. does not provide large forces during cylindrical grasp. b. cannot secure properly small cylinders because of self collision. d. cannot secure properly small object in the palm. e. a standard finger is not strong enough to oppose to three fingers. f. the opposing finger is specially designed, decreasing modularity but providing proper opposition and the optimal telemanipulation.

The selected design uses four fingers in the *f* configuration (Fig. 3). The other configurations were discarded based on the grasps analysis or on the ease of telemanipulation.

For fine manipulation, the shape of the fingertips is playing a key role. In figure 4, several shapes are compared with respect to rolling, maximum load and the ability to pick up small objects. The Dexhand is using a variable curvature with a flat end fingertip shape.

### C. Architecture

The Dexhand system is developed together with a robotic arm (Dexarm) designed and realized by Selex Galileo ([www.selex-sas.com](http://www.selex-sas.com)). The complete system architecture is represented in figure 17.

The hand has 12 DOFs, distributed in 4 modular fingers with 3 degrees of freedom each. Figure 9 presents the CAD



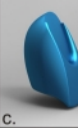

	Square	Hemi-spherical	Variable curvature	Variable curvature flat end
Finger tip shape				
Small object picking	+++	-	++	++
Rolling	--	+++	++	++
Maximum load on the finger tip during pinch grasp	++	-	+	+++

Fig. 4. Decision table for the evaluation of different fingertip geometries. (+ is positive, - is negative)

model and figure 8 shows the first finger module without housing. The actuation system is based on geared motors followed by a tendon transmission system (cf. section II). The motors are controlled using a combination DSP/FPGA. Joint torque measurements realized based on full strain gauge sensors. Multiple temperature sensors are available to protect the system against overheating and freezing. The control system of the hand is *entirely* running in the hand. The Dexhand is required to communicate over a CAN bus with a common VxWorks communication controller. The communication from the base station to the hand is routed through a real-time VxWorks system. It will allow the hand and the arm controllers to be tightly synchronized.

## II. MECHANICAL STRUCTURE

In the Dexhand, modular fingers are used in order to increase the system reliability. Indeed, with less parts, it is easier to extensively test the modules. It also improves the cost efficiency of the project. However, based on a kinematic analysis and the experience from the DLR Hand II, a modified finger is used for the thumb. As shown in [7], the thumb deserves a special treatment in order to increase the hand capabilities. For example, in order to properly oppose to the other fingers the thumb should have at least twice the maximum fingertip force. The Dexhand fingers are design to actively produce a fingertip force of 25 N (for the stretched finger it corresponds to about 3kg at finger tip<sup>1</sup> while withstanding 100 N passively.

The transmission system is using polymer Dyneema tendons and harmonic drives in order to bring the motor torque to the joints. The concept keeps the extremities (the fingers) without electronics to improve shielding and robustness. The shielding strategy consists in housing the whole electronic system in an conductive aluminum shell at least 2mm thick.

This leads to a fully EMI (Electromagnetic Influence) sealed hand body containing: the drives, the power electronics and the communication electronics. The only exceptions are the torque sensors, based on strain gauges, and some

temperature sensors, which have to be placed in the fingers. The cardanic metacarpophalangeal (MP) base joint is driven by two motors. Due to the coupling of the tendons in the MP joint the two motor torques can be used together for one DOF of the base joint. This aspect opens the possibility of using the same motors for the base joint and the proximal interphalangeal (PIP) joint. Indeed, due to the difference of lever length the required torques are scaled appropriately. The PIP joint has a fixed coupling with the distal interphalangeal joint (DIP) with a ratio of 1:1. In figure 5 joint positions and definitions are shown, the link lengths are 40, 30, and 23 mm.

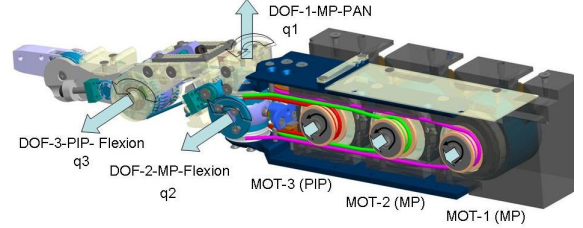


Fig. 5. Actuation principle of the fingers

The coupling matrix  $P$ , which relates motor velocity  $\dot{\theta}$  with joint velocity  $\dot{q}$  is:

$$\dot{\theta} = P\dot{q} \quad (1)$$

$$P = \frac{1}{r_p} \begin{bmatrix} r_1 & r_2 & 0 \\ -r_1 & r_2 & 0 \\ r_{13} & r_{23} & r_3 \end{bmatrix} \quad (2)$$

Where  $r_p$  is the motor pulley radius,  $r_1$ ,  $r_2$  and  $r_3$ , are the joint pulley radius, and  $r_{13}$  and  $r_{23}$  are the pulley radius of the PIP tendons in the base. Given that the coupling matrix is not configuration dependant, the relationship can be integrated in:

$$\theta = Pq \quad (3)$$

This linear relationship implies that it is possible to compute the required  $\theta$  given a desired  $q$  with a simple matrix product.

The motor unit for Dexhand has been developed based on the DLR / Robodrive ILM 25 motor including the gearing of a harmonic drive HFUC 8 with a transmission ratio of 100:1. The whole unit fits into a cylinder of 27 mm diameter and a length of 17.5 mm with a weight of 46g (Fig. 6).

The unit provides a continuous torque of 2.4 Nm with peaks up to 9 Nm which is the maximum peak torque of the gearing. In the Dexhand, the motor has been electronically limited to 2 Nm not to exceed the maximum current.

Each actuated joint has a reference mark in the middle of its motion range. A reference mark consists of a small magnet and a Hall-effect sensor located in the actuated joint. The reference marks are used to initialize the joint positions at power-up since no absolute position sensors are available. The marks can further be used to detect failures by comparing the estimated joint position and the signal of the reference marks. The joint torque measurement is

<sup>1</sup>It is comparable to a human adult, see [8]

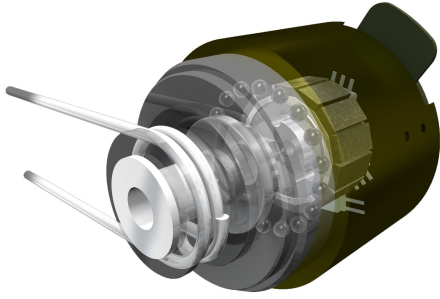


Fig. 6. Drive unit with ILM 25 and harmonic drive gearing

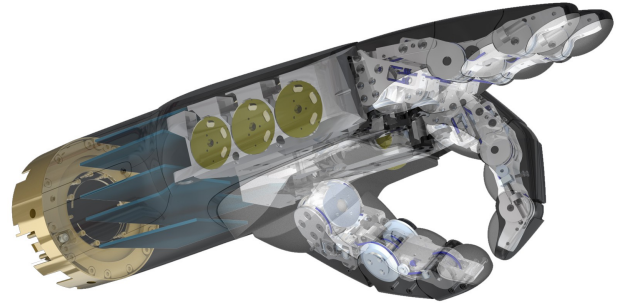


Fig. 9. Section view of Dexhand

implemented using a sensing body and a full strain gauges bridge (Fig. 7) of 5kOhm sensors. Each finger uses 3 torque sensors and therefore provides a very good sensitivity to external forces. The torque sensors are all physically located in the proximal finger link. Therefore, the sensor for the PIP/DIP-joints measures the reaction torque of the coupling tendons.

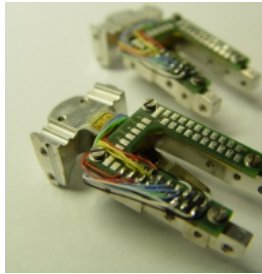


Fig. 7. Strain gauge sensor body constituting the base of the metacarpal joint

All sensors, except one of the reference sensors of the MP joint, are located in one part. This part also contains the pull relief of the wires, as well as the shield connection of the cable from the fingers to the electronics in the palm. This simplifies the assembly and the maintenance of the finger. Special care was taken in the design of the sensor body in order to prevent temperature drift.

The palm structure consists of 11 main segments. These

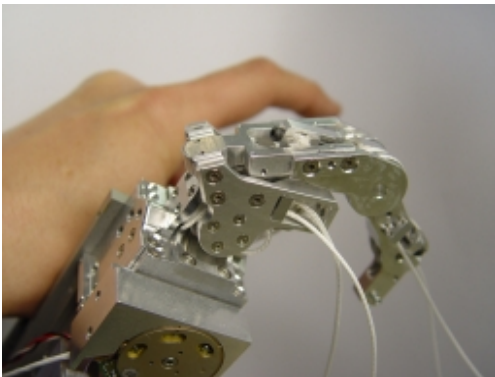


Fig. 8. Finger without housing

segments are massive aluminum parts to improve heat transfer and increase the thermal inertia. The modules of the Dexhand are four different ensembles representing the ring-, middle-, index- and thumb finger actuation units. A unit includes the tendon guidances from the motor pulleys to the MP Joint. The Palm surface mainly consists of the outer shell parts. Furthermore, all parts are designed without sharp edges. They are optimized for ideal thermal allocation and minimum resistivity (Fig. 9).

The wrist houses all electronic parts. This includes the analog, the digital and power circuit boards. The electronic boards are coupled to the palm assembly with connectors. The housing of the wrist is composed of 2 mm aluminum shells. It is fully closed to provide EMI protection.

### III. ELECTRONICS

The design of outer space capable electronics faces 4 main challenges:

- radiation tolerance
- heat dissipation (no convection)
- size/performance
- power limitation

Parts that are readily available for radiation duty are, in general, larger and have less performance than their industrial equivalents. One can expect to use only mature technologies, meaning 10, if not 20 years old. However, based on the successful results of the ROKVISS experiment [9], in which mostly standard automotive parts have been successfully used in outer space for more than 5 years. It has been decided to use the same strategy and to perform system level tests to control the results. Moreover, designing a human sized hand with 12 active joints requires both high-performance and small electronic components. This is not feasible with radiation tolerant parts only. Therefore, the existing off-the-shelf solutions have been evaluated focusing on the possible usability for outer space applications. The chosen motor controller components have been successfully tested in a rad-test-facility under a 120 Gy irradiation<sup>2</sup>. The Dexhand prototypes will not be equipped with radiation tolerant components. However, the DSP, the FPGA and D-RAM

<sup>2</sup>120 Gy is equivalent to the irradiation dose when staying 20 year outside of the ISS with a 2mm shielding

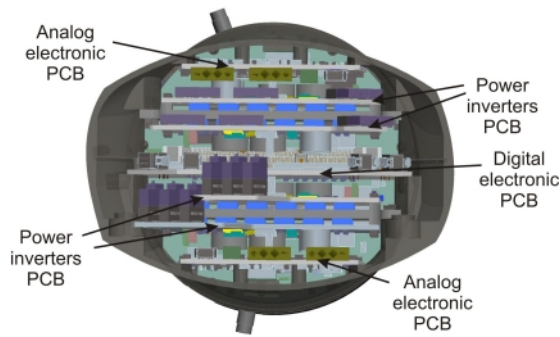


Fig. 10. PCB placement in the hand base (view from palm to wrist)

used in the Dexhand are, in size and function, equivalent to the radiation tolerant counterparts. The resulting board packaging is shown in fig. 10.

All the PCBs are functionally divided directly behind the mechanical hand connector. The input filter board absorbs noise coming from the hand carrier and ensures that the hand device does not inject any spikes in the carrier. The power supply board, which additionally behaves as a backplane to connect all horizontal PCBs of the stack, provides: total power limitation, soft-start, hot plugging circuitry and signal conditioning. Four horizontal PCBs connect each one finger with three motors. Two other horizontal PCBs are used for analog signal conversion of the strain gauges sensors. Figure 11 shows the main digital electronic PCB which carries the DSP, the FPGA, the flash memory and the different RAMs.



Fig. 11. Main digital PCB containing DSP, FPGA, flash memory, D-RAM and M-RAM

The cables and connectors to connect the fingers and the motor units to the PCBs have been specially designed for this project. Those connectors are completely shielded and combine power lines and signal cables (see Fig.12). The connector includes a screwed mechanical fixation to ensure proper connection after the vibrations of the launch process.

The power distribution in the Dexhand is reported in presented in fig. 13.

Due to the absence of convective heat exchange, heat transfers are only the result of conduction<sup>3</sup> and radiation.

<sup>3</sup>Even though attached to the wrist of the DexArm only a limited amount of heat may be transferred.

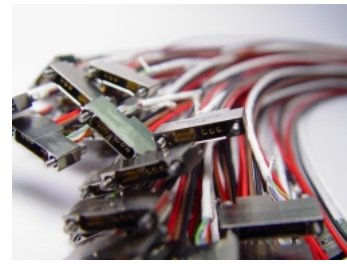


Fig. 12. Special connectors including power and signal cables

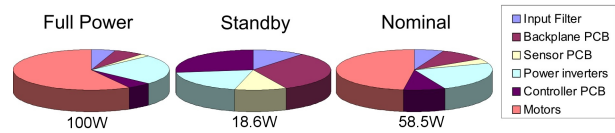


Fig. 13. Power distribution in the Dexhand depending on the operating case

Therefore, terrestrial design patterns can not be used directly (no heat sink, no fan). The losses due to the motors are not an important issue since they can be modulated by the software, slowing down and limiting the current for example. Those losses are limiting the maximum operation time, imposing cooling periods once the maximal operational temperature is reached. The communication electronics and the digital circuits are more important because they can not easily be switched off. They define the relaxation behavior of the Dexhand. Thermal simulation results, in the case of a nominal operation during 1749 seconds, are depicted in Fig. 14. The Dexhand is assumed to be isolated at the wrist interface and to receive radiated power only from the sun and the ISS.

#### IV. SOFTWARE AND CONTROL

As presented in the previous section, the hand is equipped with a DSP and a FPGA. The FPGA is used for low level, functional blocks as depicted in Fig. 15. In the DSP, functional blocks such as calibration tables, impedance control loops, communication and safety systems are implemented (Fig. 16). The controller itself is an impedance controller designed to run at 1kHz.

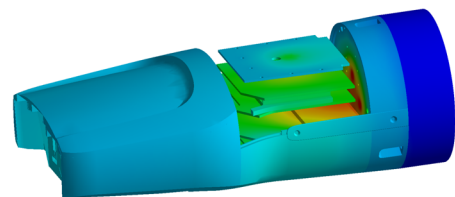
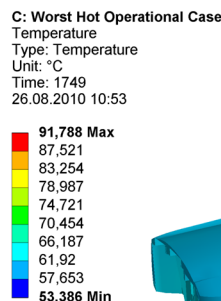


Fig. 14. Thermal behaviour after 1749 secondes of nominal operation. The hottest point is located on the DSP (in the digital electronic board)

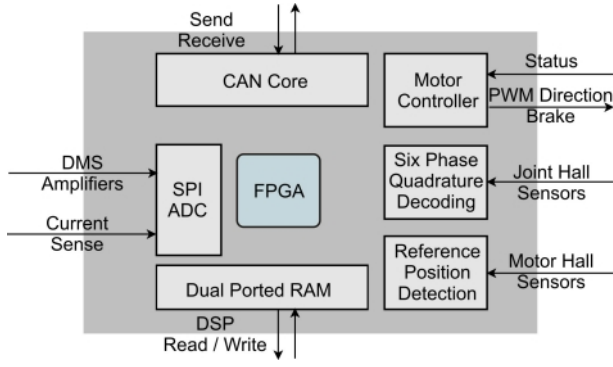


Fig. 15. Functions implemented in the FPGA

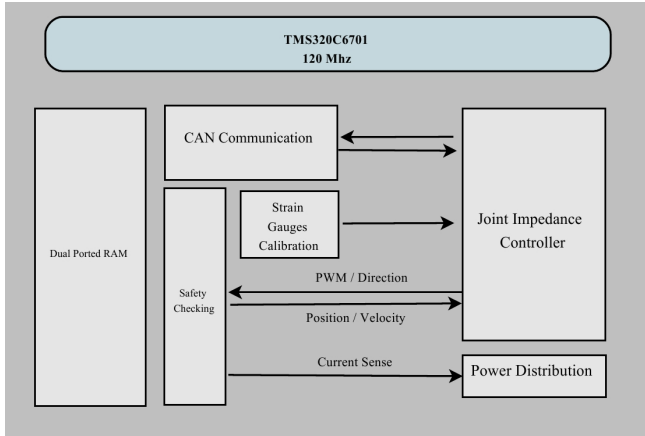


Fig. 16. Functions implemented in the DSP

### A. Software

The communication to the system (Fig. 17) is done via CAN bus, on which no hard real time data is allowed. The commands to the system are always asynchronous. However, in the case of a telemanipulation scenario, the real-time system VxWorks machine is used to establish the data exchange between the data glove data source and the Dexhand. The VxWorks system is used to monitor the communication bus and provide a TCP/IP communication interface from any standard operating system.

### B. Control

In order to set the joint position of the fingers, while controlling the applied joint torques, a joint impedance controller is used. Table I reports the variable definitions.

The dynamics model of the finger is:

$$M(q)\ddot{q} + C(\dot{q}, q) + G(q) = \tau_{friction} + \tau_m + \tau_{ext} \quad (4)$$

Where all quantities are expressed in the joint coordinates and are transformed in motor coordinates using the coupling matrix  $P$  (see Sec. II):

$$\dot{\theta} = P\dot{q} \quad (5)$$

Using the principle of virtual works:

$$\tau_q = P^T \tau_\theta, \tau_\theta = P^{-T} \tau_m \quad (6)$$

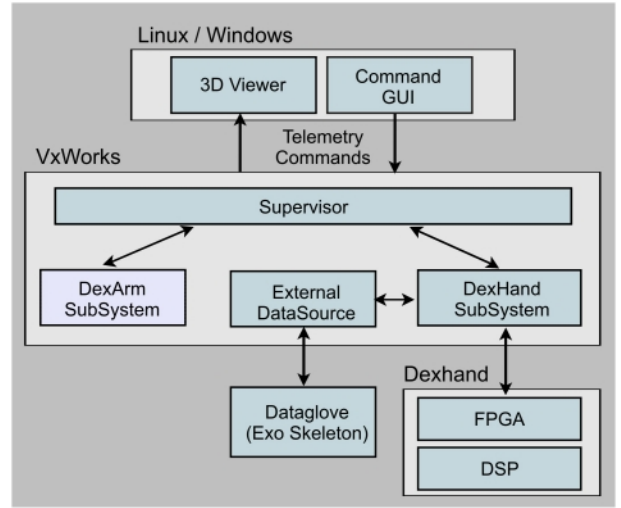


Fig. 17. Communication Architecture

TABLE I  
VARIABLE DEFINITION

Symbol	Unit	Description
$q$	rad	measured joint position
$q_{des}$	rad	desired joint position
$\theta$	rad	measured motor position
$\theta_{des}$	rad	desired motor position
$\tau_q$	Nm	commanded joint torque
$\hat{\tau}_q$	Nm	estimated joint torque
$\tau_\theta$	Nm	motor torque
$K_{imp}$	Nm/rad	prescribed joint stiffness
$K_\tau$		torque tracking gain
$\tau_{ext}$	Nm	joint torque due to external forces
$\tau_m$	Nm	joint torque produced by the motor
$\tau_{grav}$	Nm	joint torque due to gravity
$\tau_{friction}$	Nm	joint torque due to friction
$M$	kg	mass matrix in joint coordinates
$C$		centrifugal and coriolis terms
$G$		gravity terms
$P$		coupling matrix

The stiffness control law can be written:

$$\tau_{imp} = K_{imp}(q - q_{des}) \quad (7)$$

$$\tau_{ref} = \tau_{imp} + \tau_{grav} + \tau_{friction} \quad (8)$$

$$\tau_m = K_\tau(\tau_{ref} - \hat{\tau}) + \tau_{ref} \quad (9)$$

Replaced in eq. (4) it yields the desired static behaviour:

$$\tau_{ext} = K_{imp}(q - q_{des}) \quad (10)$$

Figure 18 shows how the finger (c.f. Fig.8) behaves during a step motion with and without collision.

### CONCLUSION

This paper presented an overview of the Dexhand project. The development is based on the experience of DLR in designing and building multi-fingered robot hands. The experience acquired with the ROKVISS project also guided many decisions.

Due to the very large design space, a methodology was required to select the design concept. The method analyzes

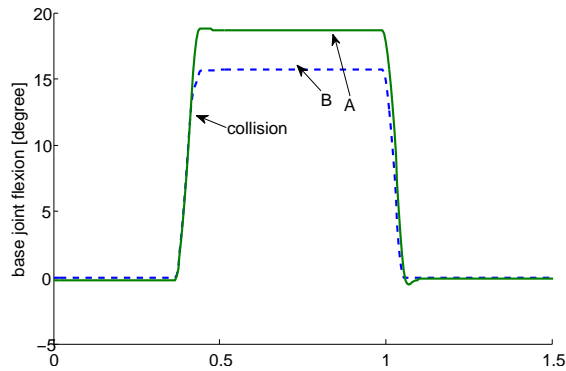


Fig. 18. Base joint flexion angle in radian. The green curve (A) is a free step motion. The blue curve is a step motion with a rigid wall impact (B). After collision, a small extra motion of the motors is allowed by the finger stiffness (the tendons and gears). Therefore, the joint angle increases slightly before equilibrium. The finger itself stops moving at impact time.

the grasps feasibility and stability to infer the required degrees of freedom. The need for tele-manipulation also drives the design toward a human like configuration of the fingers.

It should be noted that the biggest issue in term of thermal control are the digital electronic circuits and not the motors or the power inverters. Indeed, they have very little dissipation capabilities.

The radiation and EMI issues are mainly solved by using a thick enclosing aluminum shell. The fingers proved to be capable of applying a 25N at the fingertip and can withstand 100N impact load. Those performances are comparable with a human adult.

The control system runs entirely in the Dexhand, allowing very low communication bandwidth requirements. The structure permits a future tight connection between the Dexarm and the Dexhand, to perform hand/arm operations.

#### ACKNOWLEDGMENT

The authors would like to thank the Dexhand team at DLR, as well as, the ESA for the opportunity to develop a EVA capable hand.

#### REFERENCES

- [1] M. A. Diftler, R. O. Ambrose, S. M. Goza, K. Tyree, and E. Huber, "Robonaut Mobile Autonomy: Initial Experiments," in *IEEE International Conference on Robotics and Automation*, Barcelona, Spain, April 2005, pp. 1437 – 1442.
- [2] B. Rubinger, M. Brousseau, J. Lymer, C. M. Gosselin, T. Laliberté, and J.-C. Piedboeuf, "A novel robotic hand - SARAHA for operations on the international space station," *Proceeding of the ASTRA 2002 Workshop*, 2002.
- [3] J. Butterfaß, G. Hirzinger, S. Knoch, and H. Liu, "DLR's multisensory hand part I: Hard- and software architecture," *Proceedings of the IEEE Int. Conf. on Robotics and Automation*, 1998.
- [4] C. Borst, M. Fischer, S. Haidacher, H. Liu, and G. Hirzinger, "DLR hand II: experiments and experiences with an anthropomorphic hand," in *ICRA*, 2003, pp. 702–707.
- [5] Z. Chen, N. Y.Lii, T. Wimboeck, S. Fan, M. Jin, C. H. Borst, and H. Liu, "Experimental study on impedance control for the five-fingered dexterous robot hand DLR-HIT II," *Proceedings - IEEE IROS*, 2010.

- [6] M. Grebenstein and P. van der Smagt, "Antagonism for a highly anthropomorphic hand arm system," *Advanced Robotics*, no. 22, pp. 39–55, 2008.
- [7] M. Chalon, T. Wimböck, M. Grebenstein, and G. Hirzinger, "The thumb: Guidelines for a robotic design," in *IROS*, 2010.
- [8] MD. Raoul Tubiana, *The Hand*. W. B. Saunders Co, 1985.
- [9] G. Hirzinger, K. Landzettel, D. Reintsema, C. Preusche, A. Albuschäfer, B. Rebele, and M. Turk, "Rokviss - robotics component verification on iss," 2005.